Microchimica Acta (2018) 185: 172
https://doi.org/10.1007/s00604-018-2717-6

ORIGINAL PAPER

Preparation of a nanocomposite material consisting of cuprous oxide, polyaniline and reduced graphene oxide, and its application to the electrochemical determination of hydrogen peroxide

Jianbo Liu[1,2] · Chen Yang[1] · Yonghui Shang[1,2] · Ping Zhang[1] · Jing Liu[1] · Jianbin Zheng[2]

Received: 11 October 2017 / Accepted: 26 January 2018 / Published online: 13 February 2018

Abstract

A method is described for the preparation of a nanocomposite material consisting of cuprous oxide/polyaniline/reduced graphene oxide (Cu_2O/PANI/rGO). Aniline was employed as both the precursor for PANI and the reducing agent for Cu^{2+} and graphene oxide. A glassy carbon electrode was modified with the nanocomposite material. Chronoamperometric studies with the modified electrode showed it to enable an efficient electroreduction of hydrogen peroxide at −0.2 V vs. saturated calomel electrode. All measurements were performed in the absence of oxygen. Figures of merit include a wide linear response range (0.8 μM to 12.78 mM) and a low limit of detection of 0.5 μM ($S/N = 3$).

Keywords Hydrothermal synthesis · Transmission electron microscopy · X-ray diffraction · Cyclic voltammetry · Nanomaterial

Introduction

There is a substantial need for altermative methods for the determination of hydrogen peroxide (H_2O_2) [1]. Many researchers pay much attention on electrochemical method [2–5]. However, the direct detection of H_2O_2 on bare electrode is not easy. Because the reduction or oxidation of H_2O_2 on bare electrode requires a high overpotential with a low response, such high overpotential usually results in interference and the low response makes it difficult to detect H_2O_2 with a low concentration. Therefore, in order to ensure a lower overpotential and a higher response, studying modified electrodes is vital. For example, Jin [6] reported a glassy carbon electrode modified with FeS nanosheets as a highly sensitive for H_2O_2 assay in 0.1 M NaOH solution. Ni [7] described a nonenzymatic amperometric method for H_2O_2 assay which used a nanocomposite consisting of Co_3O_4 nanoparticles and mesoporous carbon nanofibers. The synergetic combination of the electrocatalytic activity of the Co_3O_4 nanoparticles and the electrical conductivity of mesoporous carbon nanofibers made the method exhibit good electrocatalytic performance in 0.1 M NaOH solution. In addition, many other metal nanoparticles [8, 9] were also employed for H_2O_2 assay. A non-enzymatic electrochemical method was obtained by modifying a glassy carbon electrode with nanocomposites containing nanoporous copper and carbon black. The result indicated that the method possessed enhanced electrocatalytic activities towards H_2O_2 assay at 0.75 V [8]. Wu [9] synthesized a sandwich structured nanocomposite consisting of mildly reduced graphene oxide modified with silver nanoparticles supported on Co_3O_4. Then, they employed such nanocomposite to fabricate a nonenzymatic electrochemical method for H_2O_2 detection. The integration of mildly reduced graphene oxide, Co_3O_4 and silver nanoparticles into a nanocomposite brought out remarkable properties to catalyze H_2O_2 with high sensitivity and wide linear range.

Electronic supplementary material The online version of this article (https://doi.org/10.1007/s00604-018-2717-6) contains supplementary material, which is available to authorized users.

✉ Jianbin Zheng
zhengjb@nwu.edu.cn

[1] College of Chemistry and Chemical Engineering, Xianyang Normal University, Xianyang, Shaanxi 712000, People's Republic of China

[2] Institute of Analytical Science/Shaanxi Provincial Key Laboratory of Electroanalytical Chemistry, Northwest University, Xi'an, Shaanxi 710069, People's Republic of China

Some transition metal oxides usually worked under high pH conditions and noble metal was expensive, which limited their wide applications. As an important semiconductor, cuprous oxide (Cu_2O) has been employed to detect H_2O_2 because of its catalytic properties and low cost [10–13]. However, the low conductivity and severe aggregation of Cu_2O limit its applications [14]. On the other hand, an appropriate supporting material possessing large surface area, high conductivity and large numbers of functional groups can prevent electrocatalytic material from aggregating and improve its conductivity [15]. Reduced graphene oxide (rGO) is a two-dimensional carbon material with large surface area and high conductivity [16]. Polyaniline (PANI) is a conductive polymer possessing excellent conductivity and large numbers of nitrogen-containing groups [17]. Therefore, the modification of rGO with PANI will enable PANI/rGO a promising support material. Some rGO/PANI-based nanocomposites were reported [18–22], in which electrochemical or chemical oxidative polymerization was employed to prepare PANI/rGO. Then, rGO/PANI-based nanocomposites were obtained by hydrothermal or other treatment. Yan [21] prepared RGO/PANI/Cu_2O via one-step in situ redox method using ethanol as the solvent. RGO/PANI/Cu_2O nanocomposites presented a flower-like structure with an average size of 2.0 μm in diameter and the product exhibits excellent microwave absorption property. The method was very simple and the product exhibits excellent microwave absorption property. However, the size of the product was big. The size of nanocomposite possessed influence on its properties and smaller size possessed larger surface area. Miao [22] synthesized Cu_2O/PANI/rGO via a one-pot method in the presence of cubic Cu_2O nanoparticles, where Cu_2O nanoparticles were synthesized first. Yan [23] reported that granular nanowires with a diameter of about 60 nm were fabricated from Cu_2O by an electrochemical method using anodic aluminium oxide as the template. This work was interesting. However, the synthesis of rGO/PANI-based nanocomposites and granular Cu_2O nanowires usually required complicate steps. Therefore, developing approaches to synthesize Cu_2O/PANI/rGO for applications is still necessary.

Here, a one-step hydrothermal method was employed to prepare Cu_2O/PANI/rGO nanocomposites. Aniline was employed as both the precursor of PANI and the reductant for Cu^{2+} and GO. The polymerization of aniline and the formation of Cu_2O and rGO occur simultaneously. After that, Cu_2O/PANI/rGO nanocomposites were employed for H_2O_2 assay. The composition, morphology and electrochemical properties of Cu_2O/PANI/rGO nanocomposite were investigated.

Experimental

Reagents and materials

Shanghai Yuanju Biotechnology (Shanghai, China, http://www.yjbiotech.cn/) supplied graphite powder, aniline (C_6H_7N, 99.9%) and $Cu(NO_3)_2{\cdot}3H_2O$. Sigma Company (http://www.sigma.com) supplied uric acid (UA), ascorbic acid (AA) and glucose (Glu). Na_2HPO_4 and NaH_2PO_4 were mixed to obtain the phosphate buffer (PB).

Apparatus

TEM images were recorded with Tecnai G^2 F20 S-TWIN (FEI, USA). D/MAX-3C (Rigaku, Japan) and TENSIR 27 (Bruker, German) were employed to record XRD patterns and FTIR spectra, respectively. CHI 660 electrochemical workstation (China) was used to measure electrochemical properties, in which glassy carbon electrode (GCE), saturated calomel electrode and platinum wire were employed as working electrode, reference electrode and counter electrode, respectively. All potentials given in thiswork were referred to the saturated calomel electrode.

Synthesis of Cu_2O/PANI/rGO

Graphite powder was employed to prepare GO through modified Hummers method [24]. 0.5 g of graphite and 0.5 g of $NaNO_3$ in 23 mL of 12.1 M H_2SO_4 were stirred in an ice bath for 15 min. Then 4.0 g of $KMnO_4$ was slowly added in an ice bath to yield a purple-green mixture. This suspension was transferred to a 40 °C water bath and magnetically stirred for 90 min. The dark brown colored paste was diluted with the slow addition of 50 mL of deionized water and allowed to stir for a further 10 min. A 6 mL portion of H_2O_2 was slowly added to quench the solution to produce a golden-brown sol. 50 mL of water was added, and the resultant product centrifuged at 5000 rpm and washed with deionized water repeatedly. Finally the product was dried at 80 °C for 24 h. Then, Cu_2O/PANI/rGO was synthesized as follows: 0.193 g $Cu(NO_3)_2{\cdot}3H_2O$ and 160 μL of aniline were added into the suspension of GO in ethanol (6.8 mg GO, 13.6 mL) under stirring. After 0.5 h, the solution was transferred into Teflon-lined autoclave (40 mL). The temperature kept at 160 °C for 360 min. When the Teflon-lined autoclave cooled, Cu_2O/PANI/rGO was centrifuged at 8000 rpm for 5 min. After the supernatant solution was removed, the precipitate was washed with deionized water. Finally the product was dried at 50 °Cfor 24 h.

Electrode modification

The casting method was employed to fabricate modified electrode. Before modifying, GCE was polished by alumina powder. Water was used for dissolution Cu_2O/PANI/rGO. Nafion was diluted with ethanol to 0.05 wt%. 6 μL of Cu_2O/PANI/rGO solution (2 mg·mL^{-1}) was dropped on electrode surface. Then 6 μL of nafion solution (0.05 wt%) was dropped on electrode surface when the solvent (water) was allowed to evaporate at ambient temperature. The modified electrode was expressed as Cu_2O/PANI/rGO/GCE. GO/GCE was fabricated in the similar way.

Results and discussion

Choice of materials

rGO attracts much attention for various applications due to its specific high surface area, exceptional electrical, mechanical, and thermal properties. PANI exhibits excellent conductivity and possesses large numbers of nitrogen-containing groups. Therefore, it is desired to employ PANI to modify rGO an advanced support material. Cu_2O is an attractive material because of its catalytic properties and low cost. Thus, decorating Cu_2O on PANI/rGO would display an excellent electrochemical activity toward H_2O_2 reduction.

Characterizations of Cu_2O/PANI/rGO

TEM and XRD are employed to characterize morphology and structure of GO and Cu_2O/PANI/rGO, respectively. Some wrinkles and folds are observed on GO nanosheet (Fig. 1a). In the case of Cu_2O/PANI/rGO (Fig. 1b, c), abundant Cu_2O nanorods are deposited on PANI/rGO. This is benefited from the large numbers of anchor sites provided by PANI/rGO. During the synthesis of Cu_2O/PANI/rGO, Cu^{2+} and GO were reduced by aniline [25, 26] and aniline was polymerized on rGO. The modification of rGO with PANI made PANI/rGO possess many functional groups. Such functional groups offer large numbers of anchor sites for the growth of dispersed Cu_2O. Moreover, the XRD pattern of Cu_2O/PANI/rGO (Fig. 1d) reveal several obvious diffraction peaks at 36.3°, 42.1°, 61.4° and 73.7°, which are indexed to (111), (200), (220) and (311) planes of Cu_2O [27]. This confirms that the nanorods decorating on PANI/rGO are Cu_2O.

The chemical composition of Cu_2O/PANI/rGO is recorded with EDS (Fig. 2a), which displays C, O, N, Cu element. FTIR spectrum characterizes chemical structures of GO and Cu_2O/PANI/rGO. Curve a in Fig. 3b displays some characteristic peaks of GO, including the stretching of −OH, −COOH, C=C, C − O at 3427, 1720, 1628 and 1082 cm^{-1}, respectively [28]. Peaks of Cu_2O/PANI/rGO at 1720 cm^{-1} and 1082 cm^{-1} almost disappears, indicating the reduction of GO [29]. Some new peaks at 627, 1292

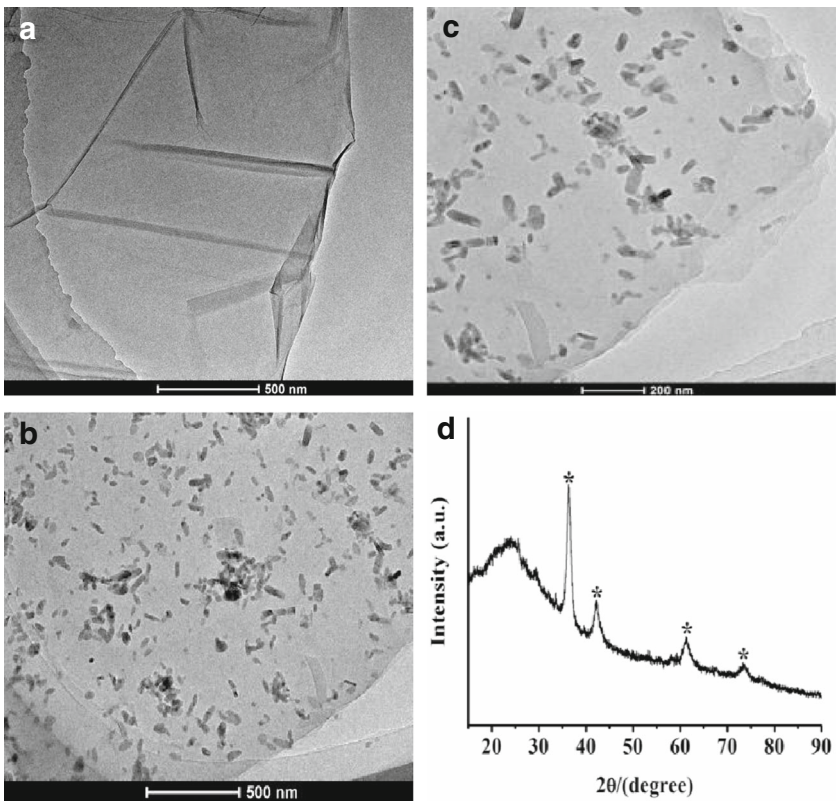

Fig. 1 TEM images of nanocomposites: **a** GO, **b**, **c** Cu_2O/PANI/rGO and XRD of (**d**) Cu_2O/PANI/rGO

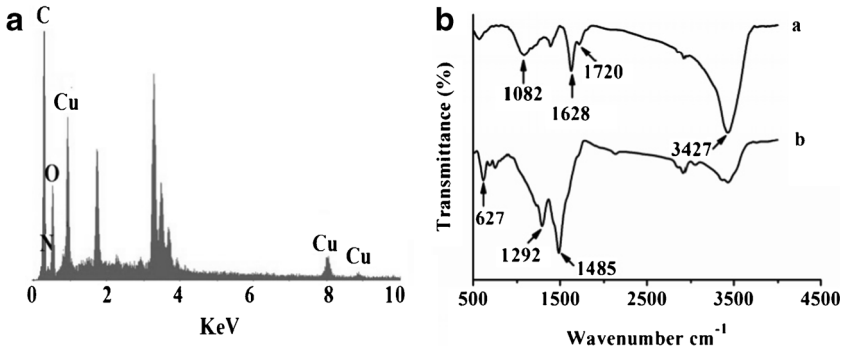

Fig. 2 **a** EDS and (**b**) FTIR spectra of Cu_2O/PANI/rGO nanocomposites

and 1485 cm^{-1} appears. These peaks relates to Cu-O vibration [30], C=C stretching of benzenoid ring and C-N stretching of secondary aromatic amine [31], respectively. Fig. S1 in the supporting information shows the raman spectroscopy of GO and rGO. rGO shows a relatively higher intensity of D to G bands than that of GO. This indicates the decrease in the size of the in-plane sp^2 domains, the removal of the oxygen functional groups in the graphene oxide nanosheets, and the reduction of GO. Two new peaks at around 212 and 634 cm^{-1} appears, which are associated with Cu_2O. From above points, Cu_2O/PANI/rGO was successfully prepared.

Electrochemical properties of Cu_2O/PANI/rGO nanocomposites

Electrochemical performance of diffirent modified electrodes was recorded with cyclic voltammograms (CVs). As shown in Fig. 3a, no electrochemical response is found on GCE (a), GO/GCE (b). However, Cu_2O/PANI/rGO/GCE (c) reveals a strong redox couple, where anodic peak is ascribed to the oxidation of Cu_2O to CuO and cathodic peak resulted from the reduction of CuO to Cu_2O [23]. In presence of H_2O_2, GCE (a') and GO/GCE (b') exhibit poor response, indicating that the direct reduction of H_2O_2 on bare electrode or GO/GCE is difficult. In the case of Cu_2O/PANI/rGO/GCE (c'), cathodic peak enhances accompanying with anodic peak current decreasing. This indicates that Cu_2O/PANI/rGO possesses excellent electrocatalytic activity toward H_2O_2 reduction. The excellent electrocatalytic activity is due to that PANI/rGO increase conductivity of Cu_2O and also prevents Cu_2O from aggregating, which provides more electroative sites for H_2O_2 reaction. The mechanism of H_2O_2 electroreduction on Cu_2O/PANI/rGO/GCE is as follows [23]:

$$Cu_2O + H_2O_2 \rightarrow 2CuO + H_2O$$
$$2CuO + 2e^- + 2H^+ \rightarrow Cu_2O + H_2O$$

Fig. S2 in the supporting information shows the response of Cu_2O/PANI/rGO/GCE in the presence of 1.0 mM H_2O_2 in phosphate buffer with various pH. The cathodic peak current enhanced firstly and then decreased with the cathodic peak shifting positively. With increasing the pH solutions, cathodic peak changes to positive values, which indicates that the redox process is pH dependence. Considering that the cathodic peak current was larger at pH 7.4. Therefore pH 7.4 phosphate buffer was chosen as the supporting electrolyte in this work.

Figure 4 displays CVs of teh modified GCE at different scan rates, which shows that the cathodic current increases with the increasing of scan rates (Fig. 4a) and a linear relationship between cathodic peak current and square root of scan rate is obtained (Fig. 4b). Therefore, electroreduction of H_2O_2 on Cu_2O/PANI/rGO/GCE is a diffusion-controlled process.

Electrocatalytic reduction of H_2O_2

Amperometric detection is an important detection method in electrochemical analysis. The resulting current is proportional to the concentration of the species generating

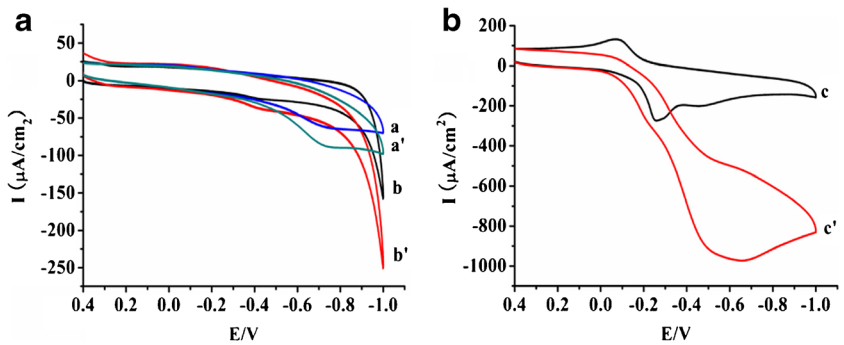

Fig. 3 Cyclic voltammograms obtained at bare GCE (**a**, a') GO/GCE (**b**, b') and Cu_2O/PANI/rGO (**c**, c') in N_2-saturated phosphate buffer (pH 7.4) in the absence (**a**, **b**, **c**) and presence (a', b', c') of 3.0 mM H_2O_2 at a scan rate of 100 mV s^{-1}

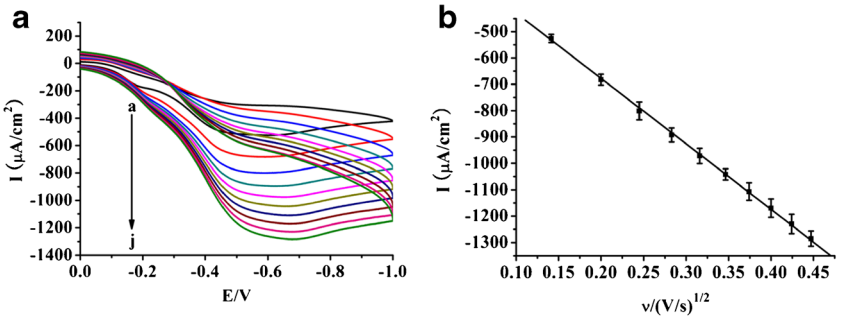

Fig. 4 **a** Cyclic voltammograms obtained at Cu_2O/PANI/rGO/GCE in presence of 3.0 mM H_2O_2 in N_2-saturated phosphate buffer (pH 7.4) at different scan rates (from a to j: 20, 40, 60, 80, 100, 120, 140, 160, 180 and 200 mV s^{-1}). **b** Linear fitting program of current versus the square root of scan rate

the current, and the quantification of H_2O_2 can be achieved via the electrochemical detection. Electrocatalytic properties of the modified GCE were studied. The reduction current of H_2O_2 obtained at working potential of of −0.2 V is higher than that of 0 V and −0.1 V. Compared with the potential of −0.3 V and −0.4 V, the background noise is low at such lower working potential. Therefore, − 0.2 V was chosen as operating potential. Because such potential was beneficial to ensure less interference and low background noise. Amperometric response current increases when H_2O_2 is added (Fig. 5a). Figure 5b reveals calibration curve. A linear regression equation of Ip (μA) = −1.376 + (−2.76)·C (mM) is obtained in the range of 0.8 μM to 12.78 mM. The sensitivity and detection limit are 39.4 μA mM^{-1} cm^{-2} and 0.5 μM (S/*N* = 3), respectively. The sensitivity is estimated from the slope of the calibration curve and electrode surface area. As shown in Table 1, many methods exhibits an excellent electrocatalytic activity toward H_2O_2 reduction. These methods have their own advantages and disadvantages. For example, the method for H_2O_2 determination based on $Ti_3C_2T_x$ is the most sensitive device described so far with a detection limit of 0.7 nM. However, $Ti_3C_2T_x$ modified GCE for H_2O_2 assay usually operated an applied potential of - 0.5 V and such operating potential may lead to more interference of other electroactive species in the solution. $Ti_3C_2T_x$ was prepared by HF treatment protocol, which made the synthesis of $Ti_3C_2T_x$ complicated. Ag nanoparticles and MnO_2 can exhibit an excellent performance to H_2O_2. However, transition metal oxides usually worked under high pH conditions and noble metal was expensive, which limited their wide applications. Comparing with other modified electrodes (Table 1), Cu_2O/PANI/rGO/GCE exhibits an excellent electrocatalytic activity toward H_2O_2 reduction with a wide linear range and a low detection limit. These benefited from the combination of Cu_2O and PANI/rGO. PANI/rGO acted as the support material and the support material provided many anchor sites for the growth of dispersed Cu_2O. Therefore, Cu_2O/PANI/rGO offered more electroative sites for H_2O_2 molecules to react. Cu_2O/PANI enhanced the conductivity of Cu_2O and thus was beneficial to improve electrocatalytic activity. However, Cu_2O/PANI/rGO/GCE possessed some limits. For example, the sensitivity was low. Therefore, further works for improving the sensitivity are on our schedule.

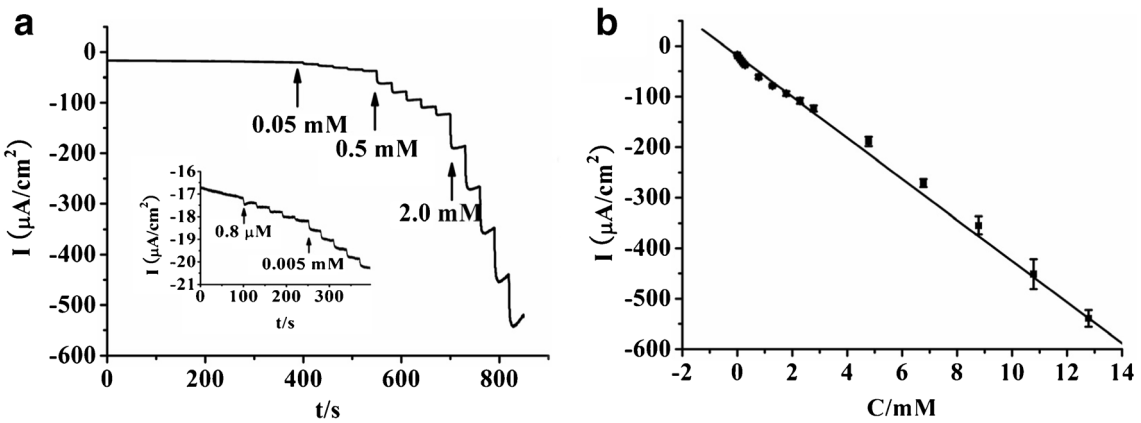

Fig. 5 **a** Amperometric curve of Cu_2O/PANI/rGO/GCE for successive additions of H_2O_2 in N_2-saturated phosphate buffer (pH 7.4) at −0.2 V. **b** Calibration curve of H_2O_2 versus its concentration

Table 1 Comparision of present work with several modified electrode for H_2O_2 detection

Electrode	Electrolyte	Applied potential (V)	Linear range (mM)	Detection limit (μM)	Sensitivity (μA mM^{-1} cm^{-2})	References
AgNPs-rGO/GCE	PB solution	−0.3	0.1–60	1.80	–	[32]
MnOOH/CC	NaOH	0.45	0.02–9.67	3.2	692.42	[33]
Nanoporous gold	PB solution	−0.4	0.01–8	3.26	–	[34]
N-graphene-Ag NDs/ITO	PB solution	−0.4	0.1–80	0.26	88.47	[3]
AuPd@GR/ITO	PB solution	−0.6	0.005–11.5	1	186.86	[4]
FeS/GCE	NaOH	−0.4	0.0005–20.5	0.15	36.36	[6]
Co_3O_4-MCNFs/Nafion/GCE	NaOH	0.2	0.001–2.58	0.5	–	[7]
Ag-Co_3O_4-rGO/GCE	PB solution	−0.3	0.0005–7	0.3	146.8	[9]
Ti_3C_2Tx/GCE	PB solution	−0.5	–	0.0035	596	[35]
Cu_2O/PANI/rGO/GCE	PB solution	−0.2	0.0008–12.78	0.5	39.4	This work

Repeatability, stability, selectivity and real sample analysis

The repeatability and stability of the Cu_2O/PANI/rGO/GCE were studied in the linear range of H_2O_2. The relative standard deviation (RSD) was 1.8% for eight successive measurements of 5 mM H_2O_2 in pH 7.4 phosphate buffer. This indicates that the modified electrode possesses good repeatability. The current responses to 5 mM H_2O_2 showed no obvious change after 30 cycles, and then decreased slowly with the increase of the number of cycles, indicating that the Cu_2O/PANI/rGO/GCE was stable. The storage stability of the method was further investigated. The amperometric measurements were measured using the same electrode and it retained above 96% of its initial response after being stored at 4 °C for 1 month. These results displayed that the modified electrode had good stability. The fabrication reproducibility of six electrodes, made independently, showed an acceptable reproducibility with the relative standard deviations of 3.5% and 4.0% for the current determination of 5 mM H_2O_2.

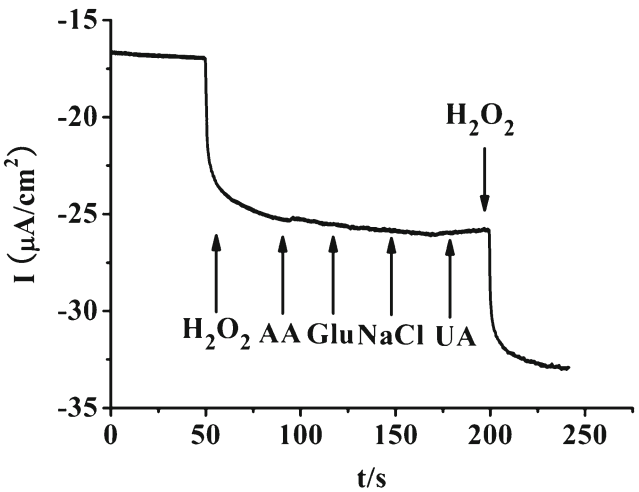

Fig. 6 Amperometric response of 0.04 mM H_2O_2, 0.01 mM AA, Glu, NaCl and UA at Cu_2O/PANI/rGO/GCE in N_2-saturated phosphate buffer (pH 7.4) at −0.2 V

Influence of AA, Glu, NaCl and UA on the detection of H_2O_2 was studied (Fig. 6). The GCE exhibits low response when AA, Glu, NaCl and UA were added, but the addition of 0.04 mM H_2O_2 shows an obvious current. The interference effects were also investigated by testing the amperometric responses of acetaminophen and dopamine (Fig. S3A). The successive addition of each interfering species brings out hardly discernible current response. These results suggest that this GCE have selectivity towards H_2O_2. It is seen obviously (Fig. S3B) that the amplitude of increase in peak current is similar in the absence and presence of air after the addition of H_2O_2. This suggests the feasibility of H_2O_2 detection in the presence of air. However, it is found that the background noise increased under air. Therefore, we used the N_2-saturated solution in order to maintain the stability of the system in the detection process.

Analysis of real samples has also been investigated. As shown in Table 2, the H_2O_2 concentration in the real sample of disinfectant containing 3.5% H_2O_2 is detected. Before experiments, the real samples were diluted with double-distilled water. It indicats that the method can be used for the H_2O_2 sample analysis.

Table 2 Determination of H_2O_2 in disinfector sample by the present method and the titration method

Sample no.	This method (μM)	RSD(%)	$KMnO_4$ titration method (μM)	RSD(%)
1	20.2	2.7	20.5	2.6
2	124.6	3.3	123.7	3.1
3	236.5	3.6	237.7	3.5

RSD (%) calculated from six measurements

Conclusions

Cuprous oxide/polyaniline/reduced graphene oxide nanocomposites were successfully synthesized by a hydrothermal approach. The experimental results revealed that Cu^{2+} and GO were reduced by aniline. Aniline was polymerized on rGO. The preparation method did not need complicated steps. PANI/rGO prevented Cu_2O from aggregating and improved its conductivity. Therefore, the method exhibited excellent electrochemical response toward H_2O_2. Cu_2O/PANI/rGO nanocomposites can be employed for H_2O_2 assay. The one-step hydrothermal approach may be extended to the fabrication of other metal oxide/conductive polymer/reduced graphene oxide nanocomposites for applications. Although Cu_2O/PANI/rGO/GCE exhibited an excellent electrocatalytic activity toward H_2O_2 reduction with a wide linear range and a low detection limit, the sensitivity was not very high, further works for improving sensitivity are on our schedule.

Acknowledgments The authors gratefully acknowledge the financial support of this project by the National Science Fund of China (NO. 21475113, 21575113), the Scientific Research Foundation of Shaanxi Provincial Key Laboratory (14JS094, 15JS100, 16JS099), the Scientific Research Foundation of Xianyang Science and Technology Bureau(2016 K02-15), and the Innovative Training Program for College Students of Xianyang Normal University(2017077).

Compliance with ethical standards

The author(s) declare that they have no competing interests.

References

1. Chen S, Yuan R, Chai Y, Hu F (2013) Electrochemical sensing of hydrogen peroxide using metal nanoparticles: a review. Microchim Acta 180:15–32
2. Zhao B, Liu Z, Fu W, Yang H (2013) Construction of 3D electrochemically reduced graphene oxide-silver nanocomposite film and application as nonenzymatic hydrogen peroxide sensor. Electrochem Commun 27:1–4
3. Tajabadi MT, Basirun WJ, Lorestani F, Zakaria R, Baradaran S, Amin YM, Sookhakian M (2015) Nitrogen-doped graphene-silver nanodendrites for the non-enzymatic detection of hydrogen peroxide. Electrochim Acta 151:126–133
4. Thanh TD, Balamurugan J, Lee SH, Kim NH, Lee JH (2016) Novel porous gold-palladium nanoalloy network-supported graphene as an advanced catalyst for non-enzymatic hydrogen peroxide sensing. Biosens Bioelectron 85:669–678
5. Alagiri M, Rameshkumar P, Pandikumar A (2017) Gold nanorod-based electrochemical sensing of small biomolecules: a review. Microchim Acta 184:3069–3092
6. Jin JY, Wu WQ, Min H, Wu HM, Wang SF, Ding Y, Yang SJ (2017) A glassy carbon electrode modified with FeS nanosheets as a highly sensitive amperometric sensor for hydrogen peroxide. Microchim Acta 184:1389–1396
7. Ni Y, Liao Y, Zheng MB, Shao SJ (2017) In-situ growth of Co_3O_4 nanoparticles on mesoporous carbon nanofibers: a new nanocomposite for nonenzymatic amperometric sensing of H_2O_2. Microchim Acta 184:3689–3695
8. Mei L, Zhang PH, Chen JY, Chen DD (2016) Non-enzymatic sensing of glucose and hydrogen peroxide using a glassy carbon electrode modified with a nanocomposite consisting of nanoporous copper, carbon black and nafion. Microchim Acta 183:1359–1365
9. Wu Q, Sheng QL, Zheng JB (2016) Nonenzymatic amperometric sensing of hydrogen peroxide using a glassy carbon electrode modified with a sandwich-structured nanocomposite consisting of silver nanoparticles, Co_3O_4 and reduced graphene oxide. Microchim Acta 183:1943–1951
10. Li Y, Zhong Y, Zhang Y, Weng W, Li S (2015) Carbon quantum dots/octahedral Cu_2O nanocomposites for non-enzymatic glucose and hydrogen peroxide amperometric sensor. Sensors Actuators B 206:735–743
11. Xu F, Deng M, Li G, Chen S, Wang L (2013) Electrochemical behavior of cuprous oxide-reduced graphene oxide nanocomposites and their application in nonenzymatic hydrogen peroxide sensing. Electrochim Acta 88:59–65
12. Liu M, Liu R, Chen W (2013) Graphene wrapped Cu_2O nanocubes: non-enzymatic electrochemical sensors for the detection of glucose and hydrogen peroxide with enhanced stability. Biosens Bioelectron 45:206–212
13. Bai HY, Zhang LQ, Shen HX, Liu LC (2017) Facile synthesis of cuprous oxide/gold nanocomposites for nonenzymatic amperometric sensing of hydrogen peroxide. Electroanalysis 29:2773–2779
14. Yang Z, Yan X, Li Z, Zheng X, Zheng JB (2016) Synthesis of Cu_2O on AlOOH/reduced graphene oxide for non-enzymatic amperometric glucose sensing. Anal Methods 8:1527–1531
15. Zhang L, Li H, Ni Y, Li J, Zhao G (2009) Porous cuprous oxide microcubes for non-enzymatic amperometric hydrogen peroxide and glucose sensing. Electrochem Commun 11:812–815
16. Shen J, Yan B, Shi M, Ye M (2011) One step hydrothermal synthesis of TiO_2-reduced graphene oxide sheets. J Mater Chem 21:3415–3421
17. Feng X, Zhang Y, Yan Z, Huang W (2014) Synthesis of polyaniline/au composite nanotubes and their high performance in the detection of NADH. J Solid State Electrochem 18:1717–1723
18. Liu P, Huang Y (2013) Synthesis of reduced graphene oxide-conducting polymers-Co_3O_4 composites and their excellent microwave absorption properties. RSC Adv 3:19033–19039
19. Liang R, Cao H, Qu M (2011) Designed synthesis of SnO_2-polyaniline-reduced graphene oxide nanocomposites as an anode material for lithium-ion batteries. J Mater Chem 21:17654–17657
20. Mohanraju K, Sreejith V, Ananth R, Cindrella L (2015) Enhanced electrocatalytic activity of PANI and $CoFe_2O_4$/PANI composite supported on graphene for fuel cell applications. J Power Sources 284:383–391
21. Yan P, Miao J, Cao J (2017) Facile synthesis and excellent electromagnetic wave absorption properties of flower-like porous RGO/PANI/Cu_2O nanocomposites. J Mater Sci 52:13078–13090
22. Miao J, Xie A, Shen Y (2016) A novel reducing graphene/polyaniline/cuprous oxide composite hydrogel with unexpected photocatalytic activity for the degradation of Congo red. Appl Surf Sci 360:594–600
23. Yan Z, Zhao J, Feng X (2013) Non-enzymatic hydrogen peroxide sensor based on a gold electrode modified with granular cuprous oxide nanowires. Microchim Acta 180:145–150
24. Perera SD, Mariano RG, Chabal Y (2012) Hydrothermal synthesis of graphene-TiO_2 nanotube composites with enhanced photocatalytic activity. ACS Catal 2:949–956
25. Muñoz-Rojas D, Oró-Solé J, Gómez-Romero P (2009) Spontaneous self-assembly of Cu_2O@PPy nanowires and anisotropic crystals. Chem Commun 39:5913–5915
26. Ju J, Chen W (2015) In situ growth of surfactant-free gold nanoparticles on nitrogen-doped graphene quantum dots for

electrochemical detection of hydrogen peroxide in biological environments. Anal Chem 87:1903–1910
27. Periasamy AP, Roy P, Chang HT (2016) Glucose oxidase and horseradish peroxidase like activities of cuprous oxide/polypyrrole composites. Electrochim Acta 215:253–260
28. Kim NH, Kuila T, Lee JH (2013) Simultaneous reduction, functionalization and stitching of graphene oxide with ethylenediamine for composites application. J Mater Chem A 1: 1349–1358
29. Li M, Huang X, Tanaka T (2012) Fabrication of two-dimensional hybrid sheets by decorating insulating PANI on reduced graphene oxide for polymer nanocomposites with low dielectric loss and high dielectric constant. J Mater Chem 22:23477–23484
30. Yang H, Ouyang J, Yu Y (2006) Electrochemical synthesis and photocatalytic property of cuprous oxide nanoparticles. Mater Res Bull 41:1310–1318
31. Goswami S, Maiti UN, Chattopadhyay KK (2011) Preparation of graphene-polyaniline composites by simple chemical procedure and its improved field emission properties. Carbon 49:2245–2252
32. Qin X, Luo Y, Sun X (2012) One-step synthesis of ag nanoparticles-decorated reduced graphene oxide and their application for H_2O_2 detection. Electrochim Acta 79:46–51
33. Xu W, Liu J, Hu C (2016) Direct growth of MnOOH nanorod arrays on a carbon cloth for high-performance non-enzymatic hydrogen peroxide sensing. Anal Chim Acta 913:128–136
34. Meng F, Yan X, Zou Z (2011) Nanoporous gold as non-enzymatic sensor for hydrogen peroxide. Electrochim Acta 56:4657–4662
35. Lorencova L, Bertok T, Dosekova E, Holazova A, Paprckova D, Vikartovska A, Sasinkova V, Filip J, Kasak P, Jerigova M, Velic D, Mahmoud KA, Tkac J (2017) Electrochemical performance of $Ti_3C_2T_x$ MXene in aqueous media: towards ultrasensitive H_2O_2 sensing. Electrochim Acta 235:471–479